Classification of CNC Vibration Speeds by Heralick Features

Melih Kuncan*
(Siirt University, Siirt, Turkey
https://orcid.org/0000-0002-9749-0418, melihkuncan@siirt.edu.tr)

Kaplan Kaplan
(Kocaeli University, Kocaeli, Turkey
https://orcid.org/0000-0001-8036-1145, kaplan.kaplan@kocaeli.edu.tr)

Yılmaz Kaya
(Batman University, Batman, Turkey
https://orcid.org/0000-0001-5167-1101, yilmaz.kaya@batman.edu.tr)

Mehmet Recep Minaz
(Siirt University, Siirt, Turkey
https://orcid.org/0000-0001-8046-6465, mehmetrecepminaz@siirt.edu.tr)

H. Metin Ertunç
(Kocaeli University, Kocaeli, Turkey
https://orcid.org/0000-0003-1874-3104, hmertunc@kocaeli.edu.tr)

Abstract: In the contemporary landscape of industrial manufacturing, the concept of computer numerical control (CNC) has emerged due to the optimization of conventional machinery, distinguished by its remarkable precision and expeditious processing capabilities. These inherent advantages have seamlessly paved the way for the pervasive integration of CNC machines across a myriad of industrial manufacturing sectors. The present study embarks upon a comprehensive inquiry, delving into the intricate analysis of a specialized prototype CNC molding machine, encompassing a meticulous assessment of its structural rigidity, robustness, and propensity for vibrational occurrences. Moreover, an insightful exploration is undertaken to discern the intricate interplay between vibrational signals and intricate machining processes, particularly under diverse conditions such as the presence or absence of the cutting tool, and at varying rotational speeds denoted in revolutions per minute (RPM). The trajectory of this research voyage encompasses an extensive array of empirical experiments meticulously conducted on the prototype CNC machine, with synchronous real-time acquisition of vibrational data. This empirical journey starts by generating two distinct datasets, each meticulously designed to encompass an assemblage of seven distinct rotational speeds, spanning the spectrum from 18000 to 30000 RPM, thereby facilitating enhanced diversity within the dataset. In parallel, a secondary dataset is meticulously derived from the CNC machine operating in the absence of the cutting tool, thereby encapsulating an exhaustive range of 20 discrete RPM values. The extraction of pivotal features aimed at discerning between the vibrational signals arising from distinct conditions (i.e., those emanating from situations involving the presence or absence of the cutting tool) and the associated variance in CNC machine speeds is facilitated through an innovative framework grounded in co-occurrence matrices. The culmination of this methodological framework is the identification of discernible co-occurrence matrices, thereby facilitating the subsequent computation of Heralick features. The classification effort was performed systematically using 10-fold cross-validation analysis, covering a number of different machine

learning models. The outcomes emanating from this intricate sequence of systematic methodologies underscore remarkable achievements. Specifically, the classification of vibrational signals corresponding to varying CNC machine speeds, contingent upon the presence or absence of the cutting tool, yields commendable accuracy rates of 94.27% and 94.16%, respectively. Notably, an exemplary accuracy rate of 100% is attained when classifying differing conditions (i.e., situations involving the presence or absence of the cutting tool) across specific RPM settings, prominently at 22000 24000 26000 28000 and 30000 RPM.

1   Introduction

In the wake of substantial advancements within the realms of science and technology in recent years, a proliferation of industrial products has materialized, accompanied by a heightened demand for innovations and novel applications across diverse domains. This burgeoning necessity for innovation has found particular resonance within the manufacturing sector, prompting a surge in research endeavors tailored to fulfill its exigencies. Among the indispensable assets within the contemporary manufacturing landscape, computer numerical control (CNC) machines have garnered widespread utilization, primarily because of their capacity to execute high-precision operations at remarkable speeds during machining processes. Consequently, the ascendancy of CNC workbenches within manufacturing operations is becoming increasingly pronounced, effectively supplanting conventional workbenches [Uyar et al., 2010, Jeong et al., 2016, Fei et al., 2019]. Of the myriad domains in which CNC machine tools are deployed prominently, mold design and manufacturing stand out as particularly prominent. This has prompted a cadre of researchers to undertake studies encompassing process modeling, mold design, dimensional and surface quality control, prototype production, and mold manufacturing, underpinned by advanced mechanical, electrical, and electronic methodologies [Imani et al., 2019, Bhogal et al., 2015, Elangovan et al., 2015]. The intricacies inherent in the machinability of numerous surfaces encountered in industrial applications stem from their intricate irregular curvature structures. The integration of 5-axis workbenches into these operations has heralded an impressive reduction in processing time, often by as much as 85%, achieved through the implementation of sophisticated cutting trajectories [Dere et al., 2019, Yurtkuran et al., 2016, Kuncan et al., 2018, Sheltami et al., 1998]. Among the merits offered by 5-axis CNC machines are heightened surface quality, flexibility in machining procedures, reduced operational duration, minimized setup requirements, and decreased operational costs. However, within the purview of recent research efforts, a salient pre-occupation has emerged: the optimization of cutting trajectories to attain the pinnacle of surface quality. Concurrently, significant emphasis is placed on the meticulous selection of optimal processing parameters, a pivotal determinant in the production of high-quality artifacts, and the delineation of parameters capable of mitigating the harmful impacts stemming from external factors [Kim et al., 2015, Du et al., 2019, Du et al., 2019]. Conversely, the evolution of technology has engendered an amplified demand for diverse CNC machines encompassing 3, 4, and 5 axes, a necessity precipitated by the expansive integration of mold manufacturing technology into diverse sectors. In recent

times, methods of mold machining have found application in various domains such as the aviation sector, automotive industry, prosthetics, footwear, tire manufacturing, and others. The ascendancy of mold manufacturing and cutting tool production has been notably underscored, with a significant proportion of these applications being rendered feasible through the use of 5-axis CNC machine tools [Khoshdarregi et al., 2014, Abuthakeer et al., 2010, Eski, 2012]. Of paramount significance within the domain of 5-axis milling lies the dual imperative of concomitantly controlling tool orientation and position during the machining of contoured and undulating surfaces. It merits attention that the intricate compositions of machine tools can contribute to anomalies within the tool, encompassing manufacturing discrepancies, assembly aberrations, quasi-static faults, and deviations in kinematic parameters. These machines evince a heightened susceptibility to angular aberrations, which can only be comprehensively defined through an accurate comprehension of the genuine kinematic nature of the machine tool. A particularly demanding sphere that requires enhanced surface quality and grapples with intricate machinability is tire manufacturing. The widespread proliferation of motor vehicle usage has translated to a substantial increase in tire consumption and demand. Within the automotive sector, a paramount parameter for the realization of vehicles characterized by diminished fuel consumption and heightened safety pertains to the judicious management of friction between the tire and the road surface.

The reduction of friction to a minimal threshold hinge on meticulous tire design and the attendant parameters. Concomitantly, the diminution of road-holding capabilities and braking distances, which are pivotal from a safety standpoint, serves to accentuate the significance of precise tire design processing. Concurrently, the facile accessibility of information regarding tire models, specifications, production dates, and origins by both dealers and consumers is deemed imperative. In this context, one noteworthy challenge pertains to the clear and consistent rendition of such information onto molds intended for diverse tire types. Broadly speaking, manufacturers operating within the tire industry require the intricate engraving of diverse patterns onto intricate molds using specialized tire pattern machines. In this context, CNC benches have emerged as indispensable tools for executing pattern engravings on molds [Kus et al., 2017, Yurdakul et al., 2016, Yan et al., 2016, Kuncan et al., 2016, Kuncan et al., 2015, Bakbak et al., 2016, Lin et al., 2012, Kuncan et al., 2018]. Chu C. H. et al. proposed a parametric methodology for the design of 3D tire molds, in which they established a foundational framework for the standardization of rubber mold design, alongside parameterizing the evolving surface model. Moreover, they introduced geometric algorithms to discern and subsequently rectify superfluous groove geometries that tend to manifest during the design process [Krishnakumar et al., 2018, Shen et al., 2019, Kaya et al., 2020]. This investigation was translated into practical implementation within a CAD/CAM system for real-time mold production. In their test samples, the authors presented a proficient approach aimed at curtailing the requisite processing time while concurrently enhancing tire quality within the paradigms of mold development and design processes [Chu et al., 2006]. In a similar vein, Chen H. C. et al. developed a computer-aided machining planning system tailored for the creation of numerical control (NC) tool paths for intricate shoe molds. The outcome of their endeavor was a transformative shift from traditional shoe mold production methodologies toward an automated production continuum. Notably, this approach facilitated the achievement of accelerated production and consistent quality outcomes through the automated

generation of tool paths. The authors emphasized the efficacy of their proposed algorithm in minimizing processing and programming editing times for the tool path, thereby optimizing overall operational efficiency [Chen et al., 2012].

In the domain of CNC machine operations, whether accompanied by tools or not, the magnitude of vibration amplitude emerges as a salient determinant of machining quality. In fact, the monitoring of vibrations has a profound import in gaging surface roughness. This critical aspect has been the subject of extensive inquiry within the pertinent literature. Plaza et al. concentrated on signal statistical value measurements, examining frequency bands inherent in vibration signals and their correlative relationship to surface roughness. In essence, the authors investigated four distinct methods for extracting signal features: power spectral density (PSD), single-spectrum analysis (SSA), time-direct analysis (TDA), and wavelet packet transformation (WPT). The outcome of their research substantiated the heightened efficacy of certain methods (SSA and WPT) in optimal extraction of vibration signals. Moreover, they underscored the pre-eminence of the WPT method as the most effective technique for real-time surface monitoring in CNC machining, distinguished by its precision, reliability, and economical computational demands [Plaza et al., 2019].

Within the framework of this research, a novel classification methodology was devised to assess the quality of machining operations across varying circumstances, encompassing conditions involving the presence or absence of a tool and distinct operational speeds. The primary objective here is to introduce an innovative classification scheme tailored for this purpose. In essence, this study entails the compilation of distinct datasets derived from a specially engineered CNC molding machine. Central to the proposed approach is a newly conceived model that harnesses the potential of co-occurrence matrices to extract Heralick features, which are integral for the classification of vibration signals. These vibration signals are meticulously collected across different conditions, pertinently encompassing scenarios with and without a tool, as well as varying operational speeds, all emanating from the specialized CNC machine tool. The empirical validation of the approach involves the use of two discrete datasets, effectively substantiating the efficacy of the proposed methodology. As a corollary to this innovative approach, the model demonstrates notable success rates in classifying vibration signals arising from various conditions and speeds. The outcomes of this study thus underscore the potential of this novel classification scheme in enhancing the comprehension and assessment of machining quality across diverse operational scenarios.

2   Related Studies

An additional study conducted by Palani and Natarajan harnessed the capabilities of an artificial neural network (ANN) model to deliver an automated, non-contact system for the flexible estimation of milled part roughness. Using a 2-D Fourier transform approach, they harnessed the ability to generate images of milled surfaces and subsequently extracted pertinent image texture features within the spatial frequency domain. Empirical outcomes demonstrated the potential for predicting the surface roughness of milled parts using the ANN method across a diverse spectrum of machining conditions. Notably, the precision of these predictions rivalled that of traditional probe-based methodologies. The authors touted the viability of their

proposed method, positing it for achieving automated surface roughness estimation with a commendable accuracy rate of 97.53% [Palani et al., 2011]. In parallel, Simon and Deivanathan embarked on an inquiry into the feasibility of pre-detecting tool wear. By examining vibration signals in the context of drilling stainless steel plates, the authors devised a technique for appraising tool performance. By leveraging statistical attributes, they achieved a notable classification of tool wear conditions, as evidenced by a success rate of 79.56% with the k-star classifier [Simon et al., 2019]. Moreover, several researchers have extended their investigations to encompass diverse machine learning methodologies beyond artificial neural networks. Caydas and Ekici, for instance, introduced three distinct variants of support vector machine (SVM) techniques, namely, least-square SVM (LS-SVM), spider SVM, and k-means SVM (SVM-KM), in tandem with an ANN model to predict the roughness values of austenitic stainless-steel surfaces in CNC processes. The input variables encompassed rotational cutting speed, feed rate, and depth of cutting. Notably, all SVM models outperformed their ANN counterparts, exhibiting robust correlations between predictive and experimental values [Çaydaş et al., 2012]. In a similar vein, Grzenda and Bustillo proposed a semi-supervised model designed to leverage partially unlabeled data, thus enhancing the precision of the model. Vibrational data coupled with roughness measurements were harnessed to bolster the accuracy of the prediction models. Their semi-supervised paradigm ingeniously employed k-nearest neighbors and random forest techniques to achieve an effective classification scheme [Grzenda et al., 2019]. Chen and Chen, in their pursuit of tool breakage detection, devised an online, process-centric monitoring system based on vibration data. This system was successfully implemented in the milling operations. The authors highlighted the comparative ease of installation and the absence of any necessary mechanism alteration, differentiating their approach from other online methods reliant on dynamometers or acoustic emission sensors. Empirical validation illustrated the practical utility of their tool break detection system across diverse cutting parameters [Chen et al., 1999].

Huang et al. introduced a hybrid tool wear prediction paradigm based on multidomain features and convolutional neural networks (CNN). They harnessed multidimensional signals encompassing 3D cutting force and vibration data to determine the health condition of tool wear. Experimental validation was performed using malfunctioning datasets procured from a high-speed CNC machine operating under milling conditions. The results underscored the notably superior prediction accuracy of the proposed method vis-à-vis alternative advanced methodologies [Huang et al., 2019]. Following a comprehensive review of the literature, it becomes evident that feature extraction and AI methodologies within the CNC machine milieu are predominantly used for predicting surface roughness accuracy or evaluating tool wear conditions [Ford et al., 2014].

3   Experimental Test Setup

This study utilized vibration data acquired from a specifically designed CNC machine tailored to produce tire sidewall molds. The operational framework of the experiments is visually outlined in Figure 1 [Kuncan et al., 2018], and the process of obtaining the vibration signals is elucidated in Figure 2. To facilitate data collection, a PCB 352C65 accelerometer sensor was strategically positioned within a dedicated aperture on the

CNC spindle motor bearing. Signal conditioners, in conjunction with the sensors, were employed to modulate and amplify the vibration signals. The signals were meticulously recorded over a duration of 10 s, employing a sampling frequency of 24 kHz facilitated by a NIDAQ 6211 data acquisition card. These acquired signals were then systematically stored within the computer's memory, subsequently culminating in the creation of comprehensive datasets.
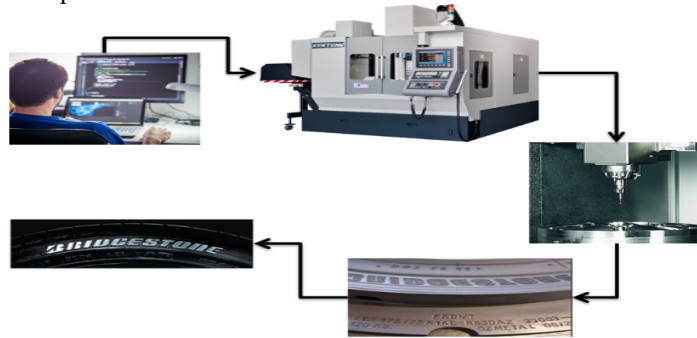

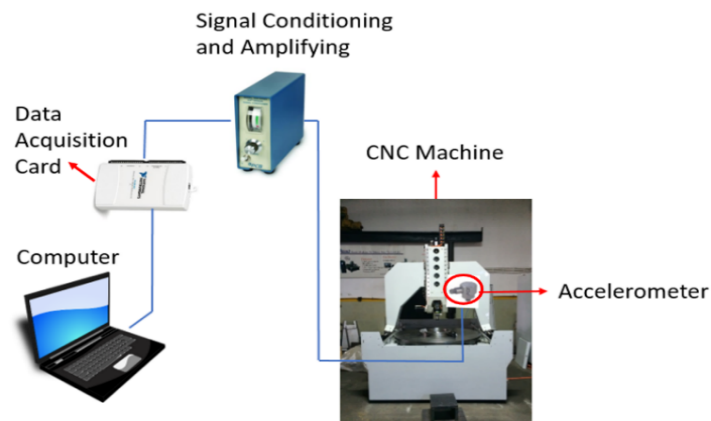*Figure 1: Schematic flow diagram of the operating system*

Figure 2: Scheme for obtaining vibration signal from CNC machine

To verify this study, two datasets were generated using vibration signals. The first dataset was obtained from the CNC mold machine with a tool that was operated at different speeds. The dataset has signals obtained at speeds of 18000, 20000, 22000, 24000, 26000, 28000, and 30000 RPM. The second dataset was obtained from the same CNC machine without a tool at 20 different speeds. The signals at different speeds with and without tools are illustrated in Figures 3–5.
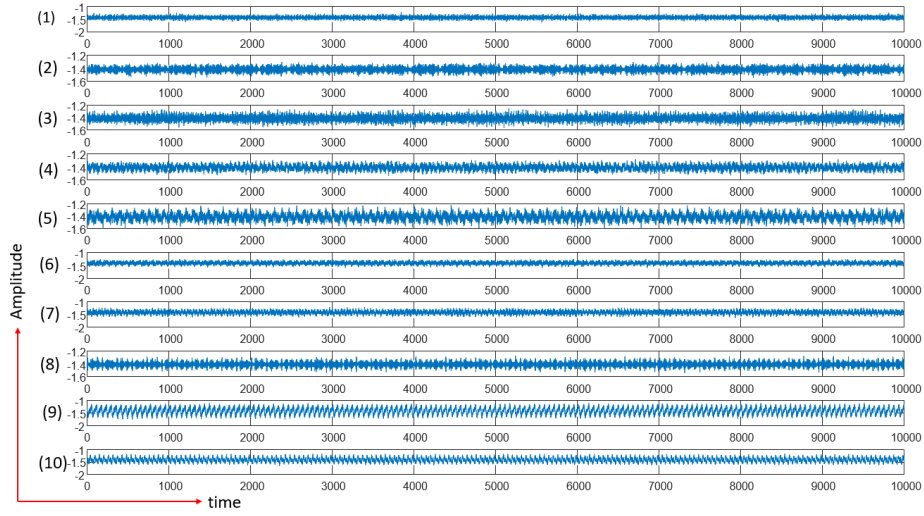
Figure 3: Signals obtained from the operation without a tool. (1) 1000 (2) 2000 (3) 3000 (4) 4000 (5) 6000 (6) 8000 (7) 10000 (8) 12000 (9) 14000 (10) 16000 RPM
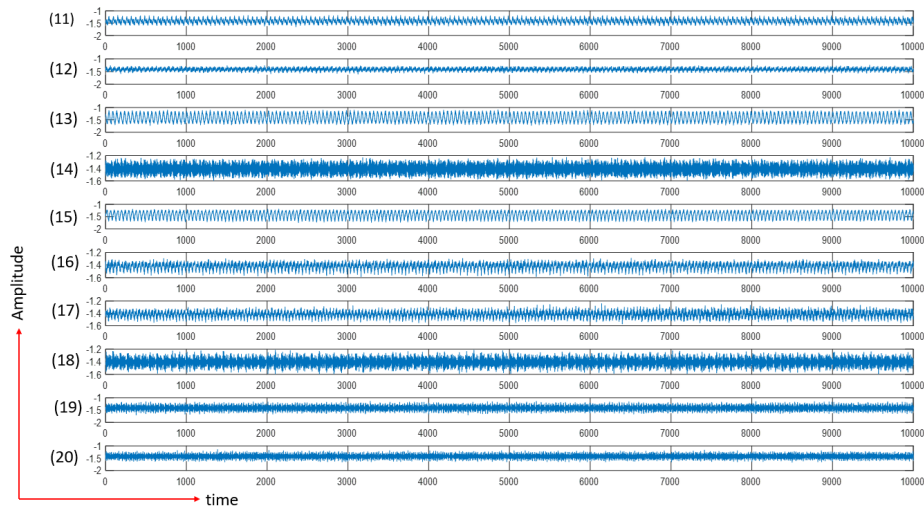

Figure 4: Signals obtained from the operation without a tool: (11) 18000 (12) 20000 (13) 22000 (14) 24000 (15) 26000 (16) 28000 (17) 30000 (18) 32000 (19) 34000 (20) 36000 RPM
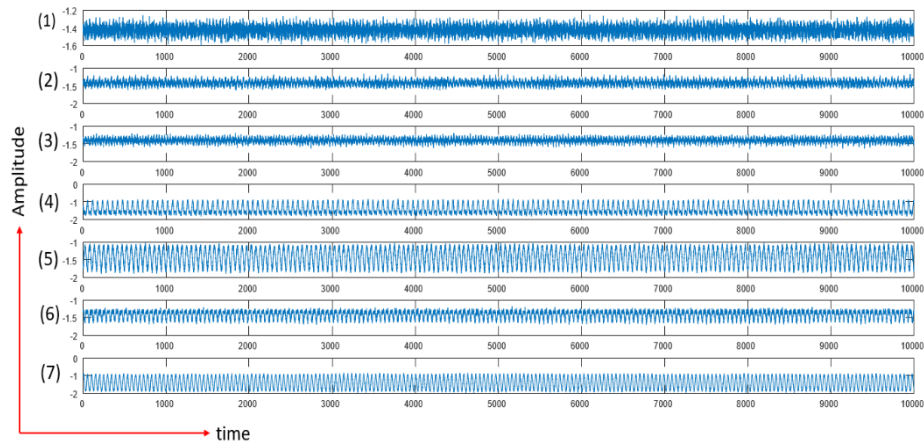
Figure 5: Signals obtained from the operation with a tool: (1) 18000 (2) 20000 (3) 22000 (4) 24000 (5) 26000 (6) 28000 (7) 30000 RPM

4   Method

This section elucidates the envisioned feature extraction methodology based on co-occurrence matrices, developed to classify CNC vibration signals garnered from various scenarios, encompassing distinct conditions involving the presence or absence of a tool, as well as varying operational speeds. The exposition starts by offering a comprehensive overview of the theoretical underpinnings of this approach, which is aptly presented through a well-defined block diagram. Subsequently, an in-depth exploration of the one-dimensional co-occurrence matrices was undertaken, furnishing a holistic comprehension of the core framework.

4.1   Proposed approach

This study proposes a new scheme for classifying vibration signals obtained from a CNC machine under different conditions. The vibration signals obtained from an industrial CNC machine were used to test the proposed approach for the cases in both the operation of the CNC machine at different speeds and in the operation of the CNC machine with or without tools. The flowchart of the proposed approach is given in Figure 6.
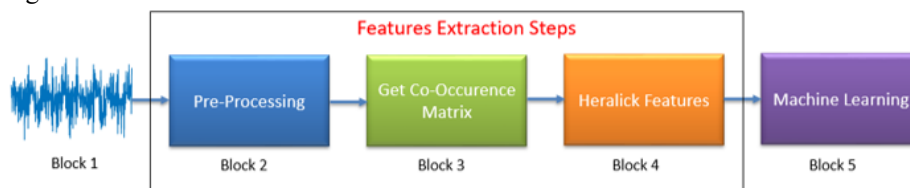

Figure 6: Signals obtained from the operation with a tool: (1) 18000 (2) 20000 (3) 22000 (4) 24000 (5) 26000 (6) 28000 (7) 30000 RPM

Figure 6 shows a meticulously designed multi-step approach to summarize the complex process of vibration signal classification. Each separate phase contributes meaningfully to the overall methodology. The specific tasks of the individual blocks are briefly described as follows:

Block 1: This initiatory stage entails the collection of vibration signals, which are systematically acquired under diverse scenarios encompassing both tool-equipped and toolless conditions, at varying speeds.

Block 2: Building upon the acquired signals, the subsequent stage entails a pivotal normalization process that culminates in their conversion into a standardized range ranging from 0 to 255. This normalization protocol, governed by Equation (1), is instrumental in rendering the signals compatible for further analyses.

$$New\ X_i = round\left(\left[\frac{X_i - Min(X)}{Max(X) - Min(X)}\right] x255\right) \tag{1}$$

The transformed signals collected at 18000 RPM under both tool and toolless conditions are visually showcased in Figure 7. A discerning observation reveals that while the form of the tool signals acquired from the CNC machine with the tool remains largely unchanged, a marked divergence becomes evident in the signals derived from the toolless machine after the transformation.

Block 3: The ensuing stage generates the calculation of co-occurrence matrices from the normalized signals. This mathematical operation, expounded upon in Section 3.2, yields matrices that encapsulate the interrelationship between signal values, which is inherently contingent upon the distance (d) parameter intrinsic to the signal.

Block 4: Within this pivotal stage, the co-occurrence matrices come into play, serving as the bedrock for extracting the Heralick features. These derived features then assume the role of input vectors, systematically channeled into machine learning models.

Block 5: Using the calculated Heralick features, the classification process is performed using the 10-fold cross-validation test. BayesNet (BN), Naive Bayes (NB), artificial neural network (ANN), logistic regression (LR), and random forest (RF) models were used to obtain performance metrics.

In summary, this comprehensive approach holistically navigates through these distinct stages, each contributing substantially to the overarching goal of classifying vibration signals. Through meticulous normalization, matrix calculations, and feature extraction, this methodology is poised to unravel the intricate complexities inherent to vibration signal analysis.
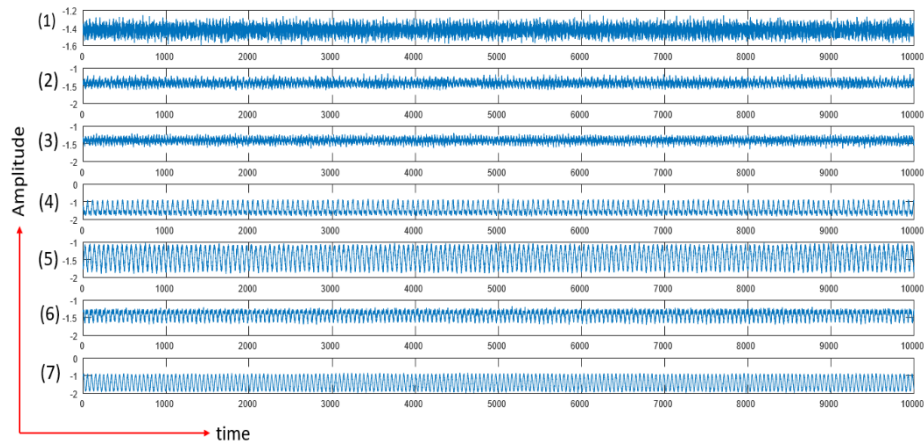
Figure 7: Conversion of signals to values in the range 0–255. (A) original signals at 18000 RPM with tools, (B) transformed signals at 18000 RPM with tools, (C) original signal at 18000 RPM without tool, (D) transformed signals at 18000 RPM without tool

4.2 Gray Level Co-Occurrence Matrices

The gray level co-occurrence matrix (GLCM) method was initially introduced by Heralick et al. in 1973 for the classification of distinct tissues [Heralick et al., 1973]. This method hinges on the notion of a gray-level dependence matrix, which is predicated on the spatial relationships among neighboring pixels within an image. Essentially, GLCM matrices are computed by evaluating the density of pixel pairs within an image that possess specific values and spatial relationships. The texture of an image is subsequently characterized by extracting statistical metrics from these matrices. In addition, GLCM furnishes second-order matrices encapsulating statistical texture features. The computation of the GLCM matrix is contingent on the distance (D) and angle (0º, 45º, 90º, and 135º) between pixels. Prior to calculating the GLCM matrix, the image is standardized to grayscale values. These matrices are pivotal in deriving the average correlation degree between pairs of pixels situated at various distances and angles. The summation of consecutive pixel counts at specified angles and distances using the GLCM matrix is subsequently mapped onto the rescaled grayscale image. Within the scope of this study, the proposed feature technique is adapted for time-series one-dimensional (1D) signals. Initially, the vibration signals undergo normalization to span the range of 0 to 255. Subsequently, GLCM matrices are computed based on these processed signals. It's worth noting that these matrices are characterized by angle values but do not incorporate distance values. A schematic representation of this method is aptly depicted in Figure 8. In Figure 8(A), imagine a signal fluctuating between four distinct pattern values (0 - 3). The co-occurrence matrix for the signal depicted in Figure 8(A) can be computed as depicted in Figure 8(B). Here #(i, j) signifies the number of instances that fulfill the specified distance condition (d = 1).
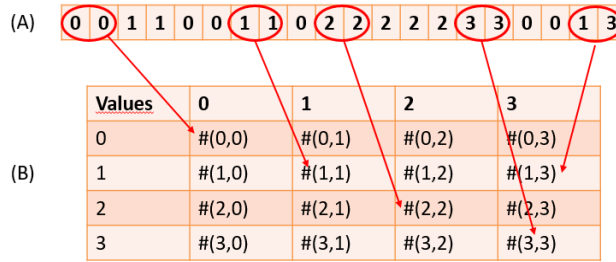
Figure 8: Process of calculating the co-occurrence matrix

Multiple co-occurrence matrices can be generated by varying the distance parameter. This parameter dictates the neighbors within the signal from which the relationships are sought. The use of the "d" parameter is elucidated in Figure 9, visually demonstrating its role and impact.
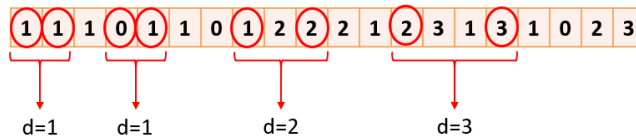
Figure 9: Usage of the d parameter

Figure 10 (A) explains how to obtain the co-occurrence matrices from a signal for different d parameters (d = {1, 2, 3 and 4}.)

(A) 0 0 1 1 0 0 1 1 0 2 2 2 2 3 3 0 0 1 3

d=1

Value	0	1	2	3
0	3	3	1	0
1	2	2	0	1
2	0	0	4	1
3	1	0	0	1

d=2

Value	0	1	2	3
0	0	4	1	1
1	3	0	1	0
2	0	0	3	2
3	2	0	0	0

(B)

d=3

Value	0	1	2	3
0	2	2	1	1
1	1	1	2	0
2	1	0	2	2
3	1	1	0	0

d=4

Value	0	1	2	3
0	3	0	1	0
1	0	2	2	0
2	1	0	1	2
3	0	1	0	1

Figure 10: Generation of identical co-occurrence matrices for different distances

Subsequently, these co-occurrence matrices undergo a normalization process. Normalization involves dividing each value within the matrix by the total number of pixels within the corresponding cell. This normalization procedure enhances the interpretability of the matrices. Using Heralick features, distinct characteristic co-occurrence matrices are derived. The 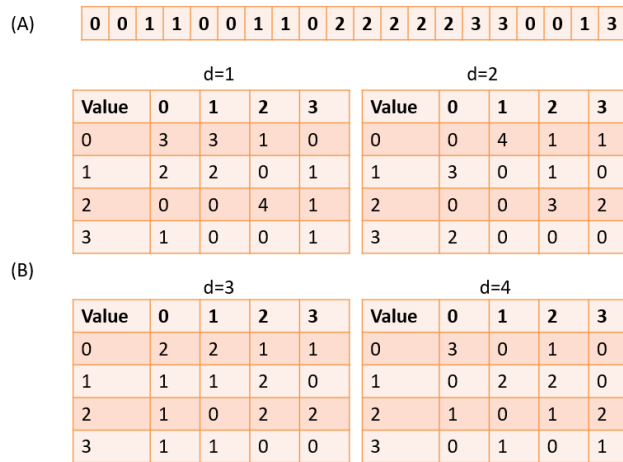computation of the Heralick features involves Equations (2) to (18), enabling the extraction of these distinctive matrix attributes.

Angular Second Moment

$$f1 = \sum_{i=1}^{N_g} \sum_{j=1}^{N_g} \left(\frac{P(i,j)}{R}\right)^2 \qquad (2)$$

Contrast

$$f2 = \sum_{n=0}^{N_g-1} n^2 \left\{ \sum_{|i-j|} \left(\frac{P(i,j)}{R}\right) \right\} \qquad (3)$$

Correlation

$$f3 = \frac{\sum_{i=1}^{N_g} \sum_{j=1}^{N_g} [ijP(i,j)/R] - \mu_x \mu_y}{\delta_x \delta_y} \qquad (4)$$

Variance

$$f4 = \sum_{i=1}^{N_g} \sum_{j=1}^{N_g} (i - \mu)^2 P(i,j) \qquad (5)$$

Inverse Different Moments

$$f5 = \sum_{i=1}^{N_g} \sum_{j=1}^{N_g} \frac{P(i,j)}{1 + (i+j)^2} \qquad (6)$$

Sum Average

$$f6 = \sum_{i=2}^{2N_g} iP_{x+y}(i) \qquad (7)$$

Sum Variance

$$f7 = \sum_{i=2}^{2N_g} (i - f_8)^2 P_{x+y}(i) \qquad (8)$$

Sum Entropy

$$f8 = -\sum_{i=2}^{2N_g} P_{x+y}(i)\log\{P_{x+y}(i)\} \qquad (9)$$

Entropy

$$f9 = -\sum_{i=1}^{N_g} \sum_{j=1}^{N_g} P(i,j)\log(P(i,j)) \qquad (10)$$

Difference Variance

$$f10 = variance\ of\ P_{x-y} \qquad (11)$$

Difference Entropy

$$f11 = -\sum_{i=0}^{N_g-1} P_{x-y}(i)\log\{P_{x-y}(i)\} \qquad (12)$$

Information Measures of Correlation

$$f12 = \frac{HXY - HXY1}{\max\{HX, HY\}} \qquad (13)$$

$$f13 = (1 - \exp[-2(HXY2 - HXY)])^{1/2} \qquad (14)$$

$$HXY = \sum_{i=1}^{N_g} \sum_{j=1}^{N_g} P(i,j) \log(p(i,j)) \qquad (15)$$

$$HXY1 = \sum_{i=1}^{N_g} \sum_{j=1}^{N_g} P(i,j) \log\{p_x(i)p_y(j)\} \qquad (16)$$

$$HXY2 = \sum_{i=1}^{N_g} \sum_{j=1}^{N_g} P_x(i)P_y(j) \log\{p_x(i)p_y(j)\}$$

$$f14 = (second\ largest\ eigenvalue\ of\ Q)^{1/2} \qquad (17)$$

Maximal Correlation
Coefficient

$$Q(i,j) = \sum_k \frac{P(i,k)p(j,k)}{P_x(i)P_y(k)} \qquad (18)$$

In Equations (2)–(18), the parameters of δx, δy, μx, μy, HX and HY are the standard deviation, means, and entropy values of Px and Py, respectively.

4.3 Performance metrics

To measure the performance rate of classification models, metrics such as accuracy, recall, precision, and f1-score were used in this study. The equations for defining the performance metrics are given in Equations (19)–(23).

$$Accuracy = \frac{TP+TN}{TP+TN+FP+FN} \qquad (19)$$

$$Error\ rate = \frac{FP+FN}{TP+TN+FP+FN} \qquad (20)$$

$$Precision = TN/(TN + FP) \qquad (21)$$

$$Recall = TP/(TP + FN) \qquad (22)$$

$$f1 - Score = (2xRecall * Precision)/(Recall + Precision) \qquad (23)$$

5   Experimental Results

The present study encompasses the acquisition of vibration data sourced from a CNC machine previously developed as a culmination of a prior investigation [Kuncan et al., 2018]. During the data acquisition phase, vibrational signals were captured through the operation of CNC machines under disparate conditions—both with and without tools—at varying rotations per minute (RPM) settings. To effectively probe the distinctive

facets of the phenomenon under examination, two discrete datasets were meticulously curated. The first dataset encompasses signals procured from the CNC machine operated with a tool across a spectrum of 7 distinct velocities, namely 18000, 20000, 22000, 24000, 26000, 28000, and 30000 RPM. The second dataset was meticulously generated through the CNC machine's operation in the absence of a tool, spanning 20 different RPM configurations.

In the preliminary phase of the study, a comprehensive analysis was conducted to discern the feasibility of distinguishing signals corresponding to varying speeds in both tool-operated and tool-less operation scenarios. The pivotal classification mechanism is underpinned using Heralick features, a set of distinctive attributes characterizing the signals. This classification framework is effectively realized using a diverse array of intelligent models, including Bayesian Network (BN), Naive Bayes (NB), Artificial Neural Network (ANN), Logistic Regression (LR), and Random Forest (RF). The evaluation of the classification models is gaged by deploying performance metrics, which is facilitated by a 10-fold cross-validation methodology leveraging the open-source Weka software platform. The salient outcomes of this performance evaluation are summarized in Table 1, which presents the achieved accuracy rates for each distinct method employed.

Vibration Signal	BN	NB	ANN	LR	RF
With tool	93.22	91.14	92.70	92.18	94.27
Without Tool	89.58	87.5	91.25	93.33	94.16

Table 1: Accuracy rates of each classification model

With reference to the informative data presented in Table 1, the endeavor of classification was executed employing an array of sophisticated models, including Bayesian Network (BN), Naive Bayes (NB), Artificial Neural Network (ANN), Logistic Regression (LR), and Random Forest (RF), each tailored to address the intricacies of datasets characterized by the presence or absence of tools. For the dataset encompassing tool-operated scenarios, the RF model emerged as particularly robust, culminating in a notable success rate of 94.27%. This achievement is the highest among the diverse classification models employed in the analysis. In stark contrast, NB model exhibited a comparatively lower success rate of 91.14%, thereby constituting a less favourable outcome in this context. A parallel observation of the dataset devoid of tool operations reveals a similar trend. Once again, the RF model showcased its potency by achieving the highest success rate of 94.16%. Conversely, the NB model, which demonstrated lower efficacy, yielded the least favourable outcome with a success rate of 87.50%.

Supplementing these insightful findings, the comprehensive evaluation of performance metrics, specifically focusing on the RF model, encompassed diverse aspects of both tool-operated and toolless operation scenarios. The intricate details of these additional performance measures are meticulously tabulated and expounded upon in Table 2, further enriching the comprehension of the outcomes achieved through the use of this model.

Vibration Signal	TP Rate	FP Rate	Precision	Recall	F-Measure
With tool	0.943	0.008	0.944	0.943	0.943
Without Tool	0.942	0.003	0.944	0.942	0.942

Table 2: Performance metrics

In the pursuit of identifying the quintessential Heralick features that wield the utmost efficacy in classifying velocities within the datasets with and without tools, an exhaustive endeavor was undertaken. This undertaking involved subjecting each distinct Heralick feature to the classification process, thereby systematically evaluating their individual contributions to the success of the classification task. The culmination of this analysis, which delineates the success rates achieved by each individual feature, is meticulously documented in Table 3.

Feature Name	With Tool	Without Tool
Angular Second Moment	39.58	25.41
Contrast	62.5	41.25
Correlation	86.98	83.33
Variance	53.12	10.83
Inverse Different Moment	73.43	37.91
Sum Average	38.54	16.875
Sum Variance	39.06	11.04
Sum Entropy	64.06	41.66
Entropy	62.5	23.95
Difference Variance	61.97	41.45
Difference Entropy	60.41	38.75
Information Measures of Correlation 1	61.45	35.00
Information Measures of Correlation 2	61.45	38.54
Maximal Correlation Coefficient	86.98	47.50

Table 3: Individual success rates of Heralick features for datasets with and without tools

Upon meticulous examination of the insights encapsulated within Table 3, it becomes evident that the features labeled as 'Correlation' and 'Maximal Correlation Coefficient' emerge as the most potent contributors to classification success. Remarkably, the deployment of only one of these features leads to an admirable success rate of 86.98%. Conversely, among the Heralick features under scrutiny, the 'Sum Average' feature demonstrates the lowest success rate, underscoring its relatively diminished efficacy within the classification framework. In alignment with the findings delineated in Table 3, it emerges that the 'Maximal Correlation Coefficient' feature stands as the pinnacle achiever in the context of the dataset without a tool, yielding an impressive success rate of 47.50%. Collectively synthesizing these observations, it becomes clear that comprehensive utilization of all Heralick features yields optimal classification performance. The datasets encompass 7 distinct speeds of vibration signals with tools and 20 diverse speeds of vibration signals without tools. A noteworthy aspect of the investigation involves the comparison of identical speeds of CNC machine rotation in the presence and absence of a tool. This meticulous analysis, aimed at discerning whether these speeds are distinguishable from each other, is exhaustively elaborated upon in Table 4. The classification process for this endeavor was meticulously executed using RF methodology.

18000 RPM	20000 RPM	22000 RPM	24000 RPM	26000 RPM	28000 RPM	30000 RPM
97.91	97.91	100	100	100	100	100

Table 4: Success rate of classification of signals with and without tools

In perusing the insights encapsulated in Table 4, a conspicuous trend emerges: a near-perfect success rate characterizes most operations conducted across distinct speeds with and without tools. However, a relatively modest success rate of 97.91% was noted solely for the datasets associated with 18000 and 20000 RPM. Considering these observations, it becomes clear that the vibrational signals emanating from diverse speeds, whether with or without tools, exhibit clear discernibility, bolstering the notion that these signals are effectively distinguishable from one another. The proposed method introduces a pivotal parameter denoted as "distance (d)," which bestows the opportunity to extract different features contingent upon varying "d" values. To discern the influence of this parameter on the classification process across datasets both with and without tools, a systematic exploration was undertaken. Different distance parameters, specifically d={1, 2, 3, 4, and 5}, were adopted to calculate the success rates. The outcomes of this comprehensive analysis, delineating the success rates corresponding to distinct "d" parameters, are thoughtfully documented in Table 5, enriching our understanding of the impact of this parameter on the classification endeavor.

d (distance)	With Tool	Without Tool
d=1	94.27	94.16
d=2	82.29	92.08
d=3	89.06	93.54
d=4	86.45	93.54
d=5	88.02	89.16
Total	95.31	95.83

Table 5: Success rate of classification of signals with and without tools

The comprehensive analysis depicted in Table 5 underscores the notable achievement of high success rates across a spectrum of distance values. This finding serves to emphasize the robustness of the proposed method in effectively distinguishing between different scenarios. Specifically, for the dataset without tools, the highest success rate of 94.16% was achieved. Notably, an even higher success rate of 95.83% was observed when all features derived from various distances were integrated, underscoring the potency of this collective approach.

Likewise, the dataset involving tool operations repeats a similar trend, with the highest success rate of 94.27% attained for the "d = 1" parameter. However, the collective employment of all features across various distances further elevated the success rate to 95.31%, substantiating the efficacy of combining these distinct features.

The synthesis of features from diverse distances emerges as a paramount strategy, yielding the most optimal classification outcomes across the spectrum of operational scenarios, thereby consolidating the robustness and effectiveness of the proposed approach.

6 Conclusions

CNC machines represent a paradigm shift stemming from the optimization of conventional machinery, which is characterized by their heightened precision and rapid processing capabilities. These attributes have led to their widespread integration within the contemporary manufacturing landscape. Of notable significance is the aspiration for reduced vibration levels among CNC users, which is a key determinant in mitigating surface roughness across workpiece materials. Consequently, the operational and idle modes of CNCs are anticipated to exhibit reasonable vibration levels, which are essential for facilitating precise and expeditious operations. Within this study, the focal point was a prototype CNC molding machine, upon which an all-encompassing investigation was embarked. This encompassed an assessment of the machine's rigidity, robustness, and vibration characteristics, effectively harnessing vibration data amassed at varying speeds. Building upon this foundational analysis, an innovative feature extraction framework was devised that is grounded in the concept of co-occurrence matrices. This ingenious approach aimed to classify vibration signals contingent upon different scenarios, encompassing the presence or absence of tools and distinct operational speeds extracted from the CNC machine.

The workflow was initiated with the normalization of vibration signal values, subsequently transforming them into a normalized range spanning 0 to 255. Thereafter, co-occurrence matrices were constructed from these recalibrated signals, forming the bedrock for calculating the Heralick features. Diverse machine learning models were then enlisted to facilitate the classification process. Each model was evaluated across disparate datasets, characterized by varying conditions and speeds, thereby affording a comprehensive assessment of the proposed approach.

The velocity of the CNC spindle motor directly affects the characteristics of the bearing spectrum. Therefore, determination of the velocity of the experimental setup plays an important role in diagnosing various faults. Because of this meticulous study, remarkable findings have emerged that prove the robustness of the proposed method. An impressive 94.27% success rate was achieved in classifying vibration signals obtained from CNC machines equipped with tools, and a similar success rate of 94.16% was attained for toolless CNC machine operations. Of particular significance is the observation that the classification of CNC machines, both with and without tools, achieved an impeccable 100% success rate at identical speeds (22000 RPM, 24000 RPM, 26000 RPM, 28000 RPM, and 30000 RPM). This collective achievement distinctly substantiates the efficacy of the proposed approach in classifying diverse vibration signals stemming from distinct tool and speed configurations.

This study has thus succeeded in delineating the acceptability of vibration levels within CNC machines under varying tool and speed contexts, while concurrently establishing the notable influence of these factors on vibration generation. These insights are of utmost relevance in deciphering the intricate interplay between vibration signals and the machining process. Looking ahead, future endeavors are poised to delve into the ramifications of diverse machining conditions on surface quality and machining efficacy, further enhancing our understanding of this intricate nexus.

References

[Abuthakeer et al., 2010] Abuthakeer, S. S., Mohanram, P. V., Kumar, G. M.: "Prediction and control of cutting Tool vibration in CNC Lathe with ANOVA and ANN." International Journal of Lean Thinking, 2(1), (2011), 1-23.

[Alghaili et al., 2016] Jeong, S. I., Jin, C. K., Seo, H. Y.: "Mold structure design and casting simulation of the high-pressure die casting for aluminum automotive clutch housing manufacturing" The International Journal of Advanced Manufacturing Technology, 84(5-8), (2016), 1561-1572.

[Bakbak et al., 2016] Bakbak, D., Ozakca, M., Gogus, M. T.: "Development of Design Methodologies for Deployable Fabric Structures in Civil Engineering" Journal of the Faculty of Engineering and Architecture of Gazi University, 31(1), (2016), 73-86.

[Bhogal et al., 2015] Bhogal, S. S., Sindhu, C., Dhami, S. S.: "Minimization of surface roughness and tool vibration in CNC milling operation" Journal of Optimization, (2015), 1-13.

[Çaydaş et al., 2012] Çaydaş, U., Ekici, S.: "Support vector machines models for surface roughness prediction in CNC turning of AISI 304 austenitic stainless steel" Journal of Intelligent Manufacturing 2012; 23(3), 2012, 639-650.

[Chen et al., 1999] Chen, J. C., Chen, W. L.: "A tool breakage detection system using an accelerometer sensor." Journal of Intelligent manufacturing, 10(2), (1999), 187-197.

[Chen et al., 2012] Chen. H. C., Yau. H. T., Lin, C. C.: "Computer-aided process planning for NC tool path generation of complex shoe molds." The International Journal of Advanced Manufacturing Technology, 58(5-8), (2012), 607-619.

[Chu et al., 2006] Chu, C. H., Song, M. C., Luo, V. C.: "Computer aided parametric design for 3D tire mold production." Computers in Industry, 57(1), (2006), 11-25.

[Dere et al., 2019] Dere, M., Filiz, I. H.: "Experimental investigation of the effects of workpiece diameter and overhang length on the surface roughness in turning of free machining steel and modelling of surface roughness by using ANFIS." Journal of the Faculty of Engineering and Architecture of Gazi University, 34(2), (2019), 676-686.

[Du et al., 2019] Du, J., Zhang, L., Gao, T.: "Acceleration smoothing algorithm for global motion in high-speed machining" Proceedings of the Institution of Mechanical Engineers, Part B: Journal of Engineering Manufacture, 233(8), (2019), 1844-1858.

[Du et al., 2019] Du, X., Huang, J., Zhu, L. M.: "Third-order chord error estimation for freeform contour in computer-aided manufacturing and computer numerical control systems." Proceedings of the Institution of Mechanical Engineers, Part B: Journal of Engineering Manufacture, 233(3), (2019), 863-874.

[Elangovan et al., 2015] Elangovan, M., Sakthivel, N. R., Saravanamurugan, S.: "Machine learning approach to the prediction of surface roughness using statistical features of vibration signal acquired in turning." Procedia Computer Science, 50, (2015), 282-288.

[Eski, 2012] Eski, İ.: "Vibration analysis of drilling machine using proposed artificial neural network predictors." Journal of mechanical science and technology, 26(10), (2012), 3037-3046.

[Fedala et al., 2018] Fedala, S., Rémond, D., Zegadi, R.: "Contribution of angular measurements to intelligent gear faults diagnosis." Journal of Intelligent Manufacturing, 29(5), (2018), 1115-1131.

[Fei et al., 2019] Fei, J., Lin, B., Yan, S.: "Modeling of surface roughness for manufactured thin-walled structure." Proceedings of the Institution of Mechanical Engineers, Part B: Journal of Engineering Manufacture, 233(4), (2019), 1216-1223.

[Ford et al., 2014] Ford, D. G., Myers, A., Haase, F.: "Active vibration control for a CNC milling machine." Proceedings of the Institution of Mechanical Engineers, Part C: Journal of Mechanical Engineering Science, 228(2), (2014), 230-245.

[Grzenda et al., 2019] Grzenda, M., Bustillo, A.: "Semi-supervised roughness prediction with partly unlabeled vibration data streams." Journal of Intelligent Manufacturing, 30(2), (2019), 933-945.

[Heralick et al., 1973] Heralick, R. M., Shanmugam, K.: "Textural features for image classification." IEEE Transactions on systems, man, and cybernetics, (6), (1973), 610-621.

[Huang et al., 2019] Huang, Z., Zhu, J., Lei, J.: "Tool wear predicting based on multi-domain feature fusion by deep convolutional neural network in milling operations." Journal of Intelligent Manufacturing, (2019), 1-14.

[Imani et al., 2019] Imani, L., Rahmani, Henzaki, A., Hamzeloo, R.: "Modeling and optimizing of cutting force and surface roughness in milling process of Inconel 738 using hybrid ANN and GA." Proceedings of the Institution of Mechanical Engineers, Part B: Journal of Engineering Manufacture, (2019), 0954405419889204.

[Jeong et al., 2016] Jeong, S. I., Jin, C. K., Seo, H. Y.: "Mold structure design and casting simulation of the high-pressure die casting for aluminum automotive clutch housing manufacturing." The International Journal of Advanced Manufacturing Technology, 84(5-8), (2016), 1561-1572.

[Kaya et al., 2020] Kaya, Y., Kuncan, M., Kaplan, K.: "Classification of bearing vibration speeds under 1D-LBP based on eight local directional filters." Soft Computing , (2020), 1-12.

[Khoshdarregi et al., 2014] Khoshdarregi, M. R., Tappe, S., Altintas, Y.: "Integrated five-axis trajectory shaping and contour error compensation for high-speed CNC machine tools." IEEE/ASME Transactions on Mechatronics, 19(6), (2014), 1859-1871.

[Kim et al., 2015] Kim, Y. J., Elber, G., Bartoň, M.: "Precise gouging-free tool orientations for 5-axis CNC machining." Computer-Aided Design, 58, (2015): 220-229.

[Krishnakumar et al., 2018] Krishnakumar, P., Rameshkumar, K., Ramachandran, K. I.: "Machine learning based tool condition classification using acoustic emission and vibration data in high speed milling process using wavelet features." Intelligent Decision Technologies, 12(2), (2018), 265-282.

[Kuncan et al., 2015] Kuncan, M., Kaplan, K., Ertunç, H. M.: "5 Axis CNC Tire Surface Prototype Machine." 3rd International Symposium On Innovative Technologies In Engineering and Science ISITES 2015, Valencia, Spain, 3-5 June, (2015), pp.759-765.

[Kuncan et al., 2016] Kuncan, M., Kaplan, K., Ertunç, H. M.: "5 Axis CNC Precision Tire Side Machining" European Journal of Technic, 6 (2), (2016), 117-123.

[Kuncan et al., 2018] Kuncan, M., Kaplan, K., Ertunç, H. M.: "Design, production and novel NC tool path generation of CNC tire mold processing machine." Journal of the Faculty of Engineering and Architecture of Gazi University, 33(3), (2018), 1183-1999.

[Kuncan et al., 2018] Kuncan, M., Kaplan, K., Ertunç, H. M.: "Experimental investigation of cutting speed on the surface roughness for CNC machine." IETS'18 International Engineering and Technology Symposium, Batman, Turkey, 3-5 May, (2018).

[Kus et al., 2017] Kus, A., Motorcu, A. R.: "Estimation of the optimum cutting parameters for surface roughness in wire electrical discharge machining of nickel based waspaloy using Taguchi method." Journal of the Faculty of Engineering and Architecture of Gazi University, 32(1), (2017), 195-204.

[Lin et al., 2012] Lin, Z., Shen, H., Gan, W.: "Approximate tool posture collision-free area generation for five-axis CNC finishing process using admissible area interpolation." The International Journal of Advanced Manufacturing Technology, 62, (2012), 1191-1203.

[Palani et al., 2011] Palani, S., Natarajan, U.: "Prediction of surface roughness in CNC end milling by machine vision system using artificial neural network based on 2D Fourier transform." The International Journal of Advanced Manufacturing Technology, 54(9-12), (2011), 1033-1042.

[Plaza et al., 2019] Plaza, E. G., López, P. N., González, E. B.: "Efficiency of vibration signal feature extraction for surface finish monitoring in CNC machining." Journal of Manufacturing Processes, 44, (2019), 145-157.

[Sheltami on et al., 1998] Sheltami, K., Bedi, S., Ismail, F.: "Swept volumes of toroidal cutters using generating curves." International Journal of Machine Tools and Manufacture, 38 (7), (1998), 855-870.

[Shen et al., 2019] Shen, X., Xie, F., Liu, X. J.: "A smooth and undistorted toolpath interpolation method for 5-DoF parallel kinematic machines." Robotics and Computer-Integrated Manufacturing, 57, (2019), 347-356.

[Simon et al., 2019] Simon, G. D., Deivanathan, R.: "Early Detection of Drilling Tool Wear by Vibration Data Acquisition and Classification." Manufacturing Letters, 21, (2019), 60-65.

[Uyar et al., 2010] Uyar, E., Kavala, D.: "5 Eksen CNC İşleme Tezgahı Tasarımı ve PC Destekli Kontrolü" 1. MakinaTek Dergisi, Turkey, (2010).

[Yan et al., 2016] Yan, Y., Zhang, L., Zhang, K.: "Corner Smoothing Transition Algorithm for Five-axis Linear Tool Path." Procedia CIRP, 56, (2016), 604-609.

[Yurdakul et al., 2016] Yurdakul, M., Gunes, S., Ic, Y. T.: "Improvement of the surface quality in the honing process using Taguchi method." Journal of the Faculty of Engineering and Architecture of Gazi University, 31 (2), (2016), 347-360.

[Yurtkuran et al., 2016] Yurtkuran, H., Korkmaz, M. E., Günay, M.: "Modelling and optimization of the surface roughness in high speed hard turning with coated and uncoated CBN insert." Gazi University Journal of Science, 29(4), (2016), 987-995.